Anonymous Referee 2:

We would like to thank the referee for the interesting and valuable comments and suggestions. RC is the referee comment and AR is the authors response. When needed, the part of the manuscript we modified or added to the old version is reported in bold. Moreover, the references of the cited literature are given in the end of the document.

Major Concerns:

RC: 1) P8, line 10 to 18: The authors mentioned that the Cv term can be estimated using AERONET observations. Given as the mass-to-extinction conversion factor is not a product provided by AERONET, it will be helpful to give some explanation and references on the methodology to obtain this parameter.

AR: The mass-to-extinction conversion factor can be obtained from the ratio of the coarse column volume concentration to the coarse mode aerosol optical thickness – i.e., υ_c/τ_c, both available on the AERONET database. The 532 nm AOT ($\tau_{c,532}$) is obtained from the coarse-mode 500 nm AOT by means of the respective Ångström exponent (AE). If a series of photometer measurements are available, the temporal average of this quantity over stable conditions can be used to get a better estimate of the needed ratio (Ansmann et al., 2012).

There are two different methods for calculating this ratio from AERONET data. Both methods make use of the aerosol size distribution to retrieve the volume of the coarse mode (Dubovik et al., 2006; Dubovik and King, 2000), and they differentiate in the way the coarse mode aerosol optical depth is calculated. The Spectral Deconvolution Algorithm (SDA) introduced by O'Neill et al. (2003) separates optically the fine and coarse mode while in the microphysical retrieval (Dubovik et al., 2006) a size threshold is invoked.

The conversion factor is central to the POLIPHON method and extended details of the AERONET data processing steps can be found in Mamouri and Ansmann (2014, 2015, 2016, 2017). Ansmann et al. (2019) further propose a methodology to derive climatological robust conversion factors. The data employed from the AERONET database are the coarse-mode volume concentration and the 500 nm AOT (denoted as extinction AOT in the database) together with the respective Ångström exponent for the 440-870 nm range. AOT and AE thresholds are used to screen out non-coarse particles and then the $\tau_{c,532}$ is estimated as described above. Finally, the climatological conversion factor is estimated.

The next few lines are inserted in the updated version of the submitting paper:

"The term c_v can be estimated using AERONET observations, being the ratio of the coarse column volume concentration (υ_c) to the coarse mode aerosol optical thickness (τ_c). More information on the different retrievals and AERONET data processing can be found in Ansmann et al. (2012), Mamouri and Ansmann (2017), and Ansmann et al. (2019)."

RC: 2) P9-10: It is clearly mentioned by the authors that the purpose of the paper is not to analyze in details these dust and volcanic events. Nevertheless, the transport analysis of the aerosols plumes should be improved. At least, it appears crucial to describe and show clearly the region impacted by the aerosols plume.

AR: Indeed, the detailed analysis of transport processes is not the main purpose of the paper. However, we agree with the referee that more information would probably be useful specifically on the horizontal extent of the plumes.

To this direction, Hysplit (Stein et al., 2015) 2-day backward trajectories are superimposed on the Figure 4 of the submitting paper (i.e., the dust SEVIRI product) that illustrate the movement of the air-masses laden with Saharan dust particles towards the EARLINET station of Finokalia (Figure 1). Furthermore, we have included an additional modeling plot (Figure2) to better display the properties of the dust event. The corresponding few lines are also added in the Page 9 Line 23 of the submitting paper:

"The extent of the dust layer at 12:00 UTC on 21 March 2018 is also evident at the WRF-CHEM dust optical depth (DOD) in Figure4b. The entire Eastern Mediterranean is affected by this episode and the simulated DOD exceeds 0.4 over certain parts of eastern Crete near the Finokalia station".

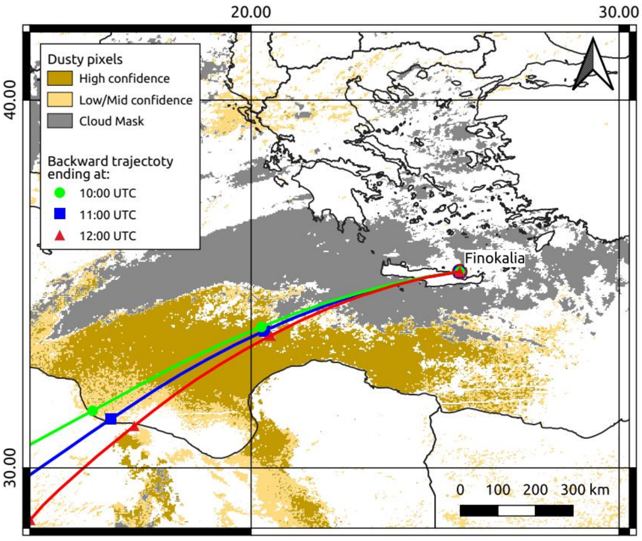

Figure 1: The dust SEVIRI product (Marchese et al., 2017) at 12:00 UTC on 21 March 2018 is represented in confidence levels (i.e., brown pixels refer to high confidence and orange pixels to mid-low confidence). The grey pixels indicate the cloud cover. Additionally, the lines indicate the 2-day Hysplit backward trajectory analysis for airmasses arriving at 4 km a.s.l. over Finokalia on 21 March 2018. The symbols show the 6 h model output.

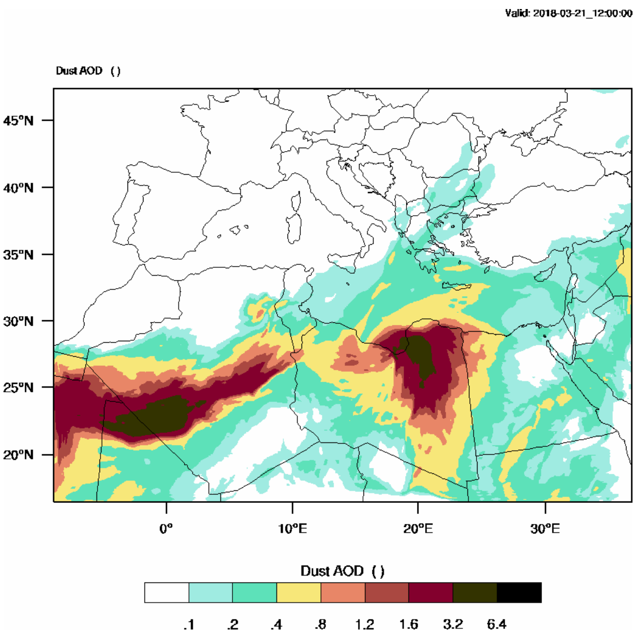

Figure 2: WRF-CHEM dust optical depth (DOD) on 21 March 2018 12:00 UTC.

Regarding the Etna dispersion case, the panel of Figure 3 shows the FLEXPART simulations of vertically integrated volcanic ash particles starting on 04:00 UTC of 30 May 2019. The output is given every 12 hours and illustrates the eastward movement of ash clouds since the eruption of Mt Etna in the early hours of 30 May. However, the detailed figure will not be included in the updated version of the submitting paper. Nonetheless, we added the following sentence in Page 10 - Line23 to better describe the event:

“As shown by the FLEXPART simulation, this plume propagated eastwards from Sicily towards the Ionian Sea, reaching parts of South Greece”.

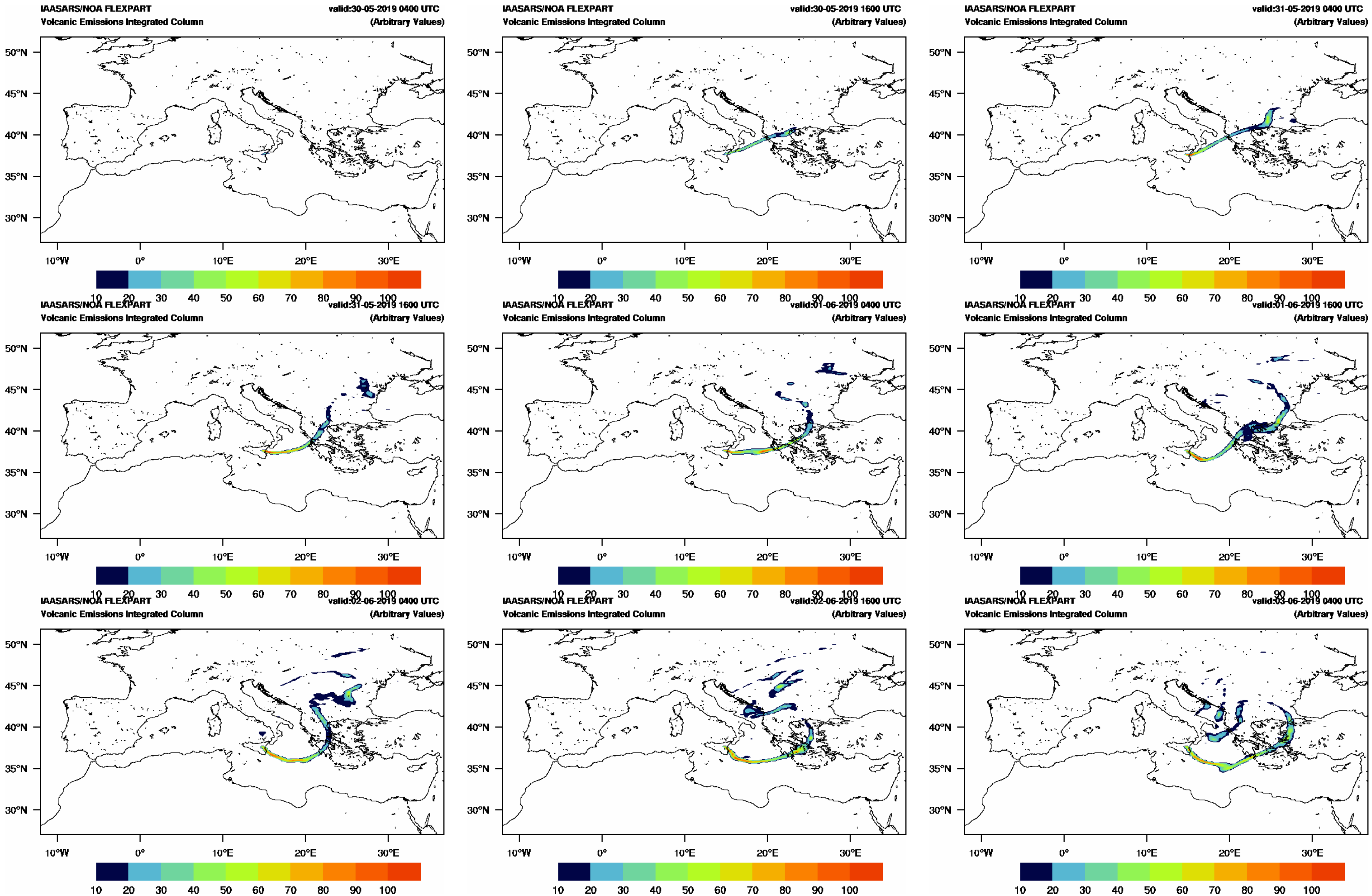

Figure 3: Volcanic ash particles simulated with FLEXPART originating from Etna, 30 May 2019, 004:00 UTC (output every 12 h).

Minor Concerns

RC: 1) P3, line 11: *"Nowadays, more than 30 stations are active and perform measurements according to the network's schedule (one daytime and two night-time measurements per week)".* It could be interesting to include a map with localization of the sites involved in the network.

AR: Figure 4 illustrates the network's geographic extent and the location of the active EARLINET stations (green squares) and the joining EARLINET stations (yellow squares) together with the non-active site of Finokalia (red square), for which lidar data are used in this study. In total, the map lists 36 active EARLINET stations, for more information see www.earlinet.org. The figure is inserted in the updated version of the submitting paper.

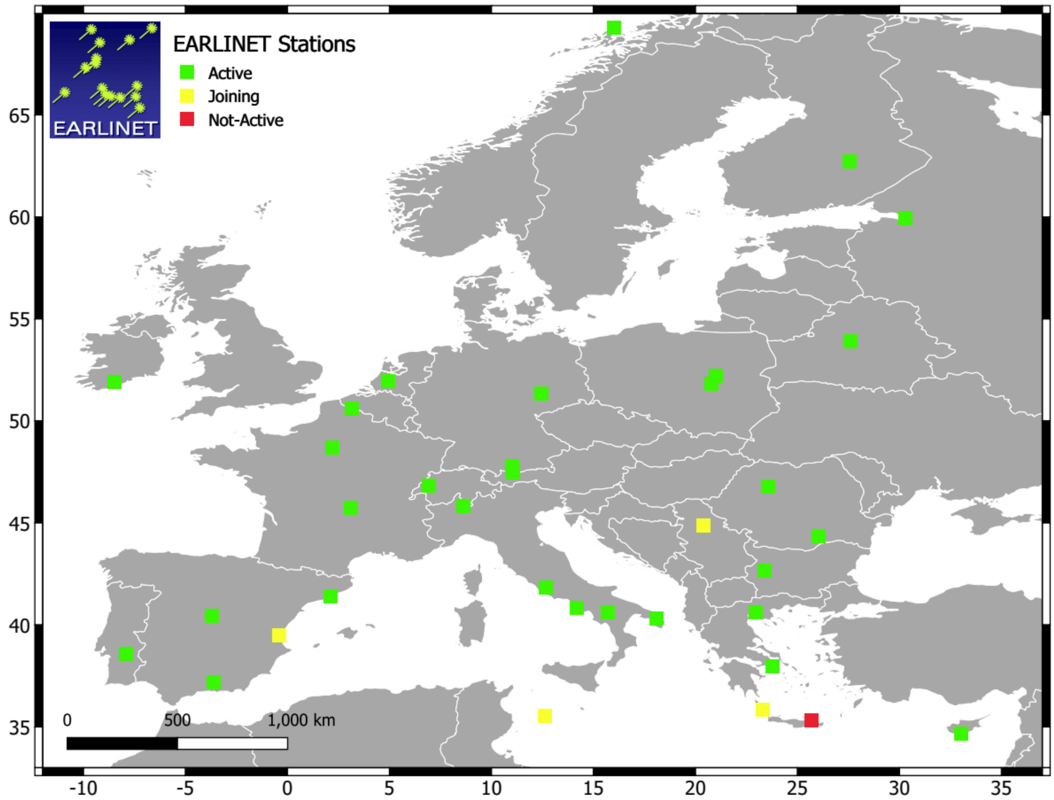

Figure 4: The EARLINET network. The green squares indicate the active stations, the yellow squares indicate the joining stations, and the red square indicates the non-active Finokalia (Greece) station.

RC: 2) P3, line 22: *"To ensure homogeneous, traceable, and quality controlled analysis of raw lidar data across the network, a centralized and fully automated analysis tool, called the Single Calculus Chain (SCC), has been developed within EARLINET".* Please, give references.

AR: The Single Calculus Chain is introduced in D'Amico et al. (2015) and is discussed in detail in the companion papers of D'Amico et al. (2016) and Mattis et al. (2016). The references are acknowledged and inserted in the updated version of the submitting manuscript:

RC: 3) P10, line 10: *"Aerosol particles of possibly volcanic origin were monitored with the multi-wavelength lidar of NOA over Antikythera, Greece".* Please, give references

AR: Tropospheric winds can advect volcanic particles, volcanic SO_2, and secondary sulfate particles from the erupting Mount Etna to the east, as it was demonstrated by Hughes et al. (2016) and Zerefos et al. (2006). The next sentence is rephrased, and the above-mentioned references are inserted in the text:

"The eastward advection of volcanic particles from Mount Etna presents a common pathway and has been previously investigated by means of active remote sensing (e.g., Hughes et al., 2016; Zerefos et al., 2006)."

RC: 4) P28: The quality of the figure 7 should be improved.

AR: We agree with the referee. Figure 5 is an improved version of the Figure 7 of the submitting paper.

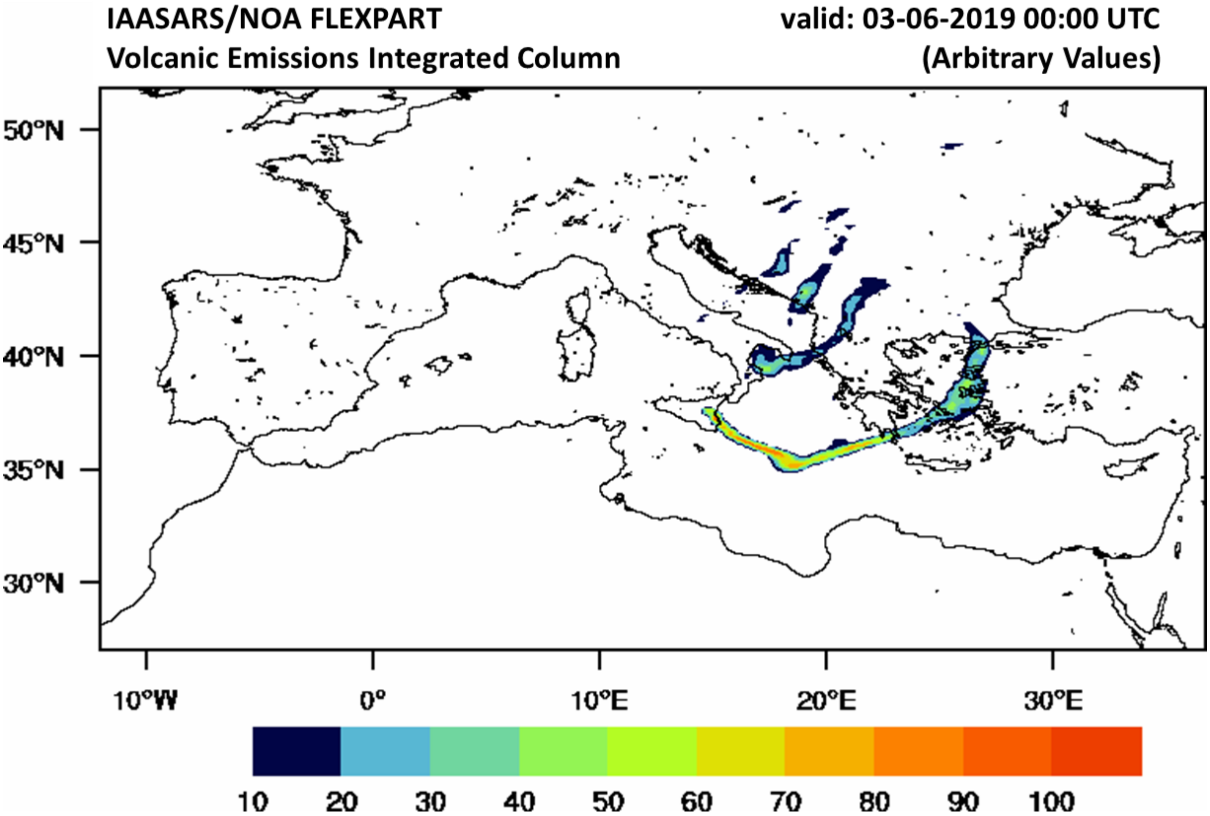

Figure 5: FLEXPART vertically integrated volcanic ash particles (arbitrary values) originating from Etna, 3 June 2019, 00:00 UTC. The green star indicates the location of Antikythera and the red line the misplacement of the simulated plume from the lidar station.

REFERENCES

Ansmann, A., Seifert, P., Tesche, M., and Wandinger, U.: Profiling of fine and coarse particle mass: case studies of Saharan dust and Eyjafjallajökull/Grimsvötn volcanic plumes, Atmospheric Chemistry and Physics, 12, 9399–9415, https://doi.org/10.5194/acp-12-9399-2012, 2012.

Ansmann, A., Mamouri, R.-E., Hofer, J., Baars, H., Althausen, D., and Abdullaev, S. F.: Dust mass, cloud condensation nuclei, and icenucleating particle profiling with polarization lidar: updated POLIPHON conversion factors from global AERONET analysis, Atmospheric Measurement Techniques, 12, 4849–4865, https://doi.org/10.5194/amt-12-4849-2019, 2019.

D'Amico, G., Amodeo, A., Baars, H., Binietoglou, I., Freudenthaler, V., Mattis, I., Wandinger, U., and Pappalardo, G.: EARLINET Single Calculus Chain–overview on methodology and strategy, Atmos. Meas. Tech., 8, 4891–4916, https://doi.org/10.5194/amt-8-4891-2015, 2015.

D'Amico, G., Amodeo, A., Mattis, I., Freudenthaler, V., and Pappalardo, G.: EARLINET Single Calculus Chain – technical – Part 1: Pre-processing of raw lidar data, Atmospheric Measurement Techniques, 9, 491–507, https://doi.org/10.5194/amt-9-491-2016, 2016.

Dubovik, O. and King, M. D.: A flexible inversion algorithm for retrieval of aerosol optical properties from Sun and sky radiance measurements, J. Geophys. Res., 105, 20673–20696, 2000.

Dubovik, O., Sinyuk, A., Lapyonok, T., Holben, B. N., Mishchenko, M., Yang, P., Eck, T. F., Volten, H., Muñoz, O., Veihelmann, B., van der Zande, W. J., Leon, J.-F., Sorokin, M., and Slutsker, I.: Application of spheroid models to account for aerosol particle nonsphericity in remote sensing of desert dust, J. Geophys. Res., 111, D11208, doi:10.1029/2005JD006619, 2006.

Hughes, E. J., Yorks, J., Krotkov, N. A., da Silva, A. M., and McGill, M.: Using CATS near-real-time lidar observations to monitor and constrain volcanic sulfur dioxide (SO_2) forecasts, *Geophys. Res. Lett.*, 43, 11,089-11,097, doi:10.1002/2016GL070119, 2016.

Mamouri, R. E. and Ansmann, A.: Fine and coarse dust separation with polarization lidar, Atmospheric Measurement Techniques, 7, 3717–3735, https://doi.org/10.5194/amt-7-3717-2014, 2014.

Mamouri, R. E. and Ansmann, A.: Estimated desert-dust ice nuclei profiles from polarization lidar: methodology and case studies, Atmos. Chem. Phys., 15, 3463–3477, https://doi.org/10.5194/acp-15-3463-2015, 2015.

Mamouri, R.-E. and Ansmann, A.: Potential of polarization lidar to provide profiles of CCN- and INP-relevant aerosol parameters, Atmos. Chem. Phys., 16, 5905–5931, https://doi.org/10.5194/acp-16-5905-2016, 2016.

Mamouri, R.-E. and Ansmann, A.: Potential of polarization/Raman lidar to separate fine dust, coarse dust, maritime, and anthropogenic aerosol profiles, Atmospheric Measurement Techniques, 10, 3403–3427, https://doi.org/10.5194/amt-10-3403-2017, 2017.

Marchese, F., Sannazzaro, F., Falconieri, A., Filizzola, C., Pergola, N., and Tramutoli, V.: An Enhanced Satellite–Based Algorithm for Detecting and Tracking Dust Outbreaks by Means of SEVIRI Data, Remote Sensing, 9, https://doi.org/10.3390/rs9060537, 2017.

Mattis, I., D'Amico, G., Baars, H., Amodeo, A., Madonna, F., and Iarlori, M.: EARLINET Single Calculus Chain – technical – Part 2: Calculation of optical products, Atmospheric Measurement Techniques, 9, 3009–3029, https://doi.org/10.5194/amt-9-3009-2016, 2016.

O'Neill, N. T., Eck, T. F., Smirnov, A., Holben, B. N., and Thulasiraman, S.: Spectral discrimination of coarse and fine mode optical depth, *J. Geophys. Res.*, 108, 4559, doi:10.1029/2002JD002975, D17, 2003.

Stein, A.F., Draxler, R.R, Rolph, G.D., Stunder, B.J.B., Cohen, M.D., and Ngan, F.: NOAA's HYSPLIT atmospheric transport and dispersion modeling system, Bull. Amer. Meteor. Soc., 96, 2059-2077, http://dx.doi.org/10.1175/BAMS-D-14-00110.1, 2015.

Zerefos, C., Nastos, P., Balis, D., Papayannis, A., Kelepertsis, A., Kannelopoulou, E., Nikolakis, D., Eleftheratos, C., Thomas, W., and Varotsos, C.: A complex study of Etna's volcanic plume from ground-based, *in situ* and space-borne observations, International Journal of Remote Sensing, 27:9, 1855-1864, DOI: 10.1080/01431160500462154, 2006.